Journal of Kerbala University , Vol. 10 No.4 Scientific . 2012

Numerical Investigation of Mixed Convection inside a Wavy Upper and Lower Surfaces Cavity

Dr. Esam M. Mohamed
Babylon Technical Institute

Abstract:

A numerical study has been performed on mixed convection heat transfer inside a square cavity with sinusoidal wavy upper and lower surfaces, the vertical walls are insulated. The lower surface was maintained at uniform temperature higher than the upper surface.

Vorticity-stream function method has been used to write the dimensionless governing equations, which consist of parabolic vorticity and energy equations that are solved by (explicit) method and elliptic stream function equation solved by successive over- relaxation method (S.O.R). The system of equations was solved using finite difference discretization. The Body Fitted Coordinate system (B.F.C) has been used with the grid generation technique to solve the flow equations because of the complexity of the upper and lower surfaces shape. Two elliptic differential equations had been solved to generate the internal grid.

In the present study, the effect of number and amplitude of undulations (λ & A) of the wavy surfaces, the Richardson number (Ri) and Grashof number (Gr) on the flow structure inside the cavity and Nusselt number of the heated wall are reported for (λ=0 to 3), (A=0, 0.02, 0.04 and 0.06), (Ri =0.01, 0.1, 1 & 10), ($Gr=10^3$,$10^{3.5}$,10^4 & $10^{4.5}$) and Pr=0.71. A two-dimensional laminar viscous non-compressible fluid flow was considered.

From the present analysis, it is found that local Nusselt number increases with increasing the number of waves of the wavy surfaces. While, the mean and local Nusselt number decreases with increasing the amplitude of undulation (A) and Richardson number (Ri) and increases with increasing the Grashof number (Gr). Higher mean Nusselt number is observed at (A=0.02 & $Gr=10^{4.5}$) at low Richardson number value (Ri=0.01). The validity of the numerical code is verified by comparison with published results.

الخلاصة

تم في هذا البحث اجراء دراسة عددية لانتقال الحرارة بالحمل المختلط داخل فجوة مربعة جداريها العلوي والسفلي متموجة مع جدارين عمودية معزولة. تم ابقاء السطح المتموج الاسفل للفجوة بدرجة حرارة منتظمة اعلى من درجة حرارة السطح المتموج العلوي. تم استخدام طريقة(الدوامية–دالة الانسياب) للتعبير عن المعادلات الحاكمة التي تتكون من معادلة قطع ناقص(Elliptic)(دالة الانسياب) حيث تم حلها باستخدام طريقة الاسترخاء(Successive Over Relaxation) ومعادلتي الدوامية والطاقة وهما قطع زائد(Parabolic) وقد تم حلهما باستخدام دالة الفروق البينة. تم تحويل المعادلات الحاكمة من معادلات تفاضلية إلى معادلات جبرية باستخدام طريقة الفروق المحددة(Finite difference). بسبب التعقيد الموجود في شكل الجدارين العلوي و السفلي للفجوة فقد تم استخدام نظام الإحداثيات المطابقة للجسم(B.F.C.) مع طريقة تكوين شبكة نقاط تمكن من حل معادلات الجريان حول الأشكال المعقدة, حيث تم تكوين شبكة النقاط الداخلية بحل معادلتين تفاضليتين من نوع القطع الناقص(Elliptic).

تم دراسة تاثير عدد تموجات السطحين العلوي و السفلي للفجوة(λ=0,1,2 & 3) و ارتفاع الموجة (A=0,0.02,0.04 & 0.06) و عدد ريتشاردسون (Ri=0.01, 0.1, 1 &10) وعدد كراشوف($Gr=10^3$, $10^{3.5}$, 10^4 & $10^{4.5}$) على كل من هيكل الجريان و انتقال الحرارة على فرض أن المائع لا انضغاطي ولزج وان الجريان طباقي ثنائي الأبعاد. وقد استخدمت قيمة واحدة لعدد برانتل(Pr=0.71). بينت النتائج إن انتقال الحرارة يتأثر بمقدار كبير نتيجة زيادة عدد الموجات وارتفاع الموجة و كذلك زيادة عدد ريتشاردسون وعدد كراشوف حيث وجد إن عدد نسلت الموضعي يزداد مع زيادة عدد الموجات بينما ينخفض عدد نسلت الكلي و الموضعي مع زيادة ارتفاع الموجة للسطحين العلوي و السفلي و زيادة عدد ريتشاردسون و يزدادان بزيادة عدد كراشوف. كما إن أعظم قيمة لعدد نسلت الكلي عند استخدام قيمة منخفضة لعدد ريتشاردسون تتحقق عند ارتفاع موجة (A=0.02) وعدد كراشوف($Gr=10^{4.5}$). تم تأكيد فعالية الطريقة العددية المستخدمة بمقارنة النتائج مع نتائج البحوث السابقة (تحت نفس الظروف) حيث كان التوافق جيد.

1-Introduction:

Thermal buoyancy forces play a significant role in forced convection heat transfer when the flow velocity is relatively small and the temperature difference between the surface and the free stream is relatively large. The buoyancy force modifies the flow and the temperature fields and hence the heat transfer rate from the surface.

Problems of heat transfer in enclosures by free convection or combined free and forced convection has been an important topic for research studies due to its occurrence in industrial and technological applications. Mixed convection occurs in many heat transfer applications such as crystal growth, electronic cooling, oil extraction, solar collectors, etc. Many experimental and numerical techniques have been proposed to tackle this problem. An experimental investigation of mixed convection flow in a lid driven cavity has been performed by [1]. A heated moving bottom wall with high Reynolds number and high Grashof number was considered. Their results indicate that the overall heat transfer rate is a very weak function of the Grashof number for the examined range of Reynolds number.

Mixed convection flow in an enclosure filled with a Darcian fluid saturated uniform porous medium in the presence of internal heat generation is numerically investigated by [2]. Their results indicate that heat transfer mechanisms and the flow characteristics inside the cavity are strongly dependent on the Richardson number. Also slight effects on the streamlines for small values of Richardson number were found. Numerical mixed convection flow study had been performed by [3], in a bottom heated square lid-driven enclosure. The results show that the effects of buoyancy are more pronounced for higher values of Prandtl number. A numerical simulation for the flow of a viscous thermally stratified fluid in a square cavity was made by [4]. The flow was driven by both the top lid and buoyancy. Later on,[5], the same investigators conducted three dimensional numerical simulation of mixed convection in a square cavity heated from the top moving wall. They observed that the heat transfer was rather insensitive to the Richardson number.

From the previous studies it is seen that there are two fields of investigations, the first one deals with the cavities with upper or lower moving surface, while the second deals with that of vertical moving surfaces. Problems of heat transfer in enclosures with non uniform surfaces have been the subject of investigations for many years, too. The implication of the effect of the number and amplitude of the wavy surfaces undulation on the flow structure and heat transfer characteristics are one of these studies, as it acts to modify the flow and the temperature fields and hence the heat transfer rate from the surfaces. Also, it is evident to remember that more of the previous studies were related only to natural convection inside wavy enclosures. A numerical study of natural convection inside a wavy cavity with adiabatic vertical walls was performed by [6]. They showed that for this particular case, the wavy surface have a significant effect on the flow and heat transfer inside the cavity through reducing the local Nusselt number. A similar trend has also been observed by [7], they have presented a numerical study of natural convection in an inclined cavity with a wavy hot wall.

Revue the previous studies indicates that there is a little researches deals with the effect of the undulation and amplitude of the wavy surfaces on the transport of energy and momentum by mixed convection. The aim of the present study is to get a numerical model to investigate the characteristics of flow and thermal fields of the laminar flow passing wavy upper and lower surfaces with adiabatic vertical walls cavity. The bottom surface is heated with uniform temperature. The study based on a full solution of Navier-Stockes and energy equations. The solution based on the method of Vorticity-Stream function. The governing equations were solved using the finite-difference formulation. The study was achieved at constant Prandtl number (Pr=0.71) and dimensionless domain parameters. The effects of Richardson number, Grashof number, number of wavy surface undulations and its amplitude on the flow structure and heat transfer characteristics are investigated. Detailed results are presented in the form of stream-lines and isotherms.

2- Physical model

The physical model considered here is shown in figure (1), along with the important geometric parameters.

It consists of a wavy upper and lower surfaces square cavity with sides of length (H). Both the side vertical walls are assumed to be adiabatic while the top and bottom walls are maintained at constant and different temperatures T_c and T_h respectively. The working fluid is assigned a Prandtl number of (0.71) throughout this investigation. All the physical properties of the fluid are assumed to be constant except density variation in the body force term of the momentum equation according to the Boussinesq approximation.

3-Mathematical formulation

Under the usual Boussinesq assumption, the governing equations for steady mixed convection flow using conservation of mass, momentum and energy can be described in dimensionless form by the following equations [8].

$$\frac{\partial U}{\partial X}+\frac{\partial V}{\partial Y}=0 \qquad \text{.....(1)}$$

$$U\frac{\partial U}{\partial X}+V\frac{\partial U}{\partial Y}=-\frac{\partial P}{\partial X}+\frac{1}{\mathrm{Re}}\left(\frac{\partial^2 U}{\partial X^2}+\frac{\partial^2 U}{\partial Y^2}\right) \qquad \text{.....(2)}$$

$$U\frac{\partial V}{\partial X}+V\frac{\partial V}{\partial Y}=-\frac{\partial P}{\partial Y}+\frac{1}{\mathrm{Re}}\left(\frac{\partial^2 V}{\partial X^2}+\frac{\partial^2 V}{\partial Y^2}\right)+Ri\cdot\theta \qquad \text{.....(3)}$$

$$U\frac{\partial \theta}{\partial X}+V\frac{\partial \theta}{\partial Y}=\frac{1}{\mathrm{Re}\cdot\mathrm{Pr}}\left(\frac{\partial^2 \theta}{\partial X^2}+\frac{\partial^2 \theta}{\partial Y^2}\right) \qquad \text{.....(4)}$$

The dimensionless variables are defined as:

$$X=\frac{x}{H},\quad Y=\frac{y}{H},\quad U=\frac{u}{U_o},\quad V=\frac{v}{U_o},\quad \theta=\frac{T-T_c}{T_h-T_c}$$

The governing parameters in the preceding equations are the Reynolds number Re, Grashof number Gr, Prandtl number Pr and Richardson number Ri, which are defined as follows:

$$\mathrm{Re}=\frac{U_o\cdot H}{\nu},\quad Gr=\frac{g.\beta_e.(T_h-T_c)H^3}{\nu^2},\quad \mathrm{Pr}=\frac{\nu}{\alpha_e},\quad Ri=\frac{Gr}{\mathrm{Re}^2}$$

The associated dimensionless boundary conditions are:

$U=0,\quad V=0,\quad \theta=1$ at the bottom wall.

$U=0,\quad V=0,\quad \theta=0$ at the top wall.

$U=0,\quad V=0,\quad \frac{\partial\theta}{\partial X}=0$ at the left and right vertical walls.

The shape of the top and bottom wavy surfaces was described by the following equation.

$$Y=A[1-\cos(2\lambda\pi X)] \qquad \text{.....(5)}$$

Where, (A) is the dimensionless height of the wave and (λ) is the number of waves.

3-1 Vorticity –stream function method:

The difficulty associated with pressure determination led to eliminate the pressure term from the two momentum equations (2&3) by cross differentiation with respect to Y and X respectively and subtraction to remove the pressure entirely which leads to a vorticity-transport equation. The vorticity (Ω) is a measure of the amount of anticlockwise rotation which the fluid possesses. In addition, using the definition of a stream function (which is a scalar quantity denoted by symbol ψ), for the steady two-dimensional flow, the problem was reduced to that of solving only two equations to obtain the stream function and the vorticity.

The definition of the dimensionless vorticity, [8]

$$\Omega = \frac{\partial V}{\partial X} - \frac{\partial U}{\partial Y} \quad \text{.....(6)}$$

The definition of the dimensionless stream function that satisfies the continuity equation (1), was given by:

$$U = \frac{\partial \psi}{\partial Y} \quad \& \quad V = -\frac{\partial \psi}{\partial X} \quad \text{.....(7)}$$

Where, $(\Omega = \frac{\omega \cdot H}{U_O})$ & $(\psi = \frac{\varphi}{H \cdot U_O})$ as ω & φ are the dimensional vorticity and stream function respectively.

Using the above definitions, the two equations of stream function (continuity equation-1) and vorticity transport of flow were written in dimensionless form, as follows:

$$\frac{\partial^2 \psi}{\partial X^2} + \frac{\partial^2 \psi}{\partial Y^2} = -\Omega \quad \text{.....(8)}$$

$$\frac{\partial \psi}{\partial Y} \cdot \frac{\partial \Omega}{\partial X} - \frac{\partial \psi}{\partial X} \frac{\partial \Omega}{\partial Y} = \frac{1}{\mathrm{Re}} \left(\frac{\partial^2 \Omega}{\partial X^2} + \frac{\partial^2 \Omega}{\partial Y^2}\right) + Ri \cdot \frac{\partial \theta}{\partial Y} \quad \text{.....(9)}$$

Also, the energy equation without heat generation is:

$$\frac{\partial \psi}{\partial Y} \cdot \frac{\partial \theta}{\partial X} - \frac{\partial \psi}{\partial X} \cdot \frac{\partial \theta}{\partial Y} = \frac{1}{\mathrm{Re} \cdot \mathrm{Pr}} \left(\frac{\partial^2 \theta}{\partial X^2} + \frac{\partial^2 \theta}{\partial Y^2}\right) \quad \text{.....(10)}$$

3-2 Body Fitted Coordinate System:

The boundary conditions are difficult to be used because of the complexity of the geometrical shape of the cavity. So a Body Fitted Coordinate System has been employed to generate the grid. This method offers generation of curvilinear coordinate system with coordinate lines coincident with the boundaries of the physical domain. So a rectangular grid and finite-difference formulation was used in the computational domain. Approximations are introduced to the partial differentials to convert the partial derivatives to finite difference expressions that are used to convert the partial differential equations to algebraic equations which are solved at discrete points within the computational domain. The points (X,Y) in the irregular physical domain and its corresponding points (ζ,η) in the regular computational domain are related. In general, Laplace's partial differential equations are used [9], as follows:

$$\frac{\partial^2 \xi}{\partial X^2} + \frac{\partial^2 \zeta}{\partial Y^2} = 0 \quad \text{.....(11)}$$

$$\frac{\partial^2 \eta}{\partial X^2} + \frac{\partial^2 \eta}{\partial Y^2} = 0 \quad \text{.....(12)}$$

The above coordinate's elliptical equations are solved in the computational domain (ζ,η) to provide the grid points locations in the physical domain (X,Y), by finite difference using Successive Over Relaxation method of iteration [10].

In order to solve the governing equations of fluid flow in the computational domain, a transformation of equations (8,9 & 10) from Cartesian coordinates to general coordinates were done using chain rule, [11]. The final representative form of the governing equations is:

$$\phi \cdot \frac{\partial \psi}{\partial \xi} + \varepsilon \cdot \frac{\partial \psi}{\partial \eta} + \alpha \cdot \frac{\partial^2 \psi}{\partial \xi^2} - 2\beta \cdot \frac{\partial^2 \psi}{\partial \xi \partial \eta} + \gamma \frac{\partial^2 \psi}{\partial \eta^2} = -\Omega \cdot J^2 \quad \text{.....(13)}$$

$$\frac{\partial \psi}{\partial \eta} \cdot \frac{\partial \Omega}{\partial \xi} - \frac{\partial \psi}{\partial \xi} \frac{\partial \Omega}{\partial \eta} = \frac{1}{\mathrm{Re} \cdot J} \left(\phi \cdot \frac{\partial \Omega}{\partial \xi} + \varepsilon \cdot \frac{\partial \Omega}{\partial \eta} + \alpha \cdot \frac{\partial^2 \Omega}{\partial \xi^2} - 2\beta \cdot \frac{\partial^2 \Omega}{\partial \xi \partial \eta} + \gamma \frac{\partial^2 \Omega}{\partial \eta^2}\right) + \frac{Ri}{J} \cdot \left(\frac{\partial Y}{\partial \eta} \cdot \frac{\partial \theta}{\partial \xi} - \frac{\partial Y}{\partial \xi} \cdot \frac{\partial \theta}{\partial \eta}\right) \quad \text{.....(14)}$$

$$\frac{\partial \psi}{\partial \eta}\cdot\frac{\partial \theta}{\partial \xi}-\frac{\partial \psi}{\partial \xi}\frac{\partial \theta}{\partial \eta}=\frac{1}{Pe\cdot J}(\phi\cdot\frac{\partial \theta}{\partial \xi}+\varepsilon\cdot\frac{\partial \theta}{\partial \eta}+\alpha\cdot\frac{\partial^2 \theta}{\partial \xi^2}-2\beta\cdot\frac{\partial^2 \theta}{\partial \xi\partial \eta}+\gamma\frac{\partial^2 \theta}{\partial \eta^2}) \quad ....(15)$$

Where:

$$\alpha=(\frac{\partial X}{\partial \eta})^2+(\frac{\partial Y}{\partial \eta})^2 \quad .....(16)$$

$$\beta=\frac{\partial X}{\partial \xi}\cdot\frac{\partial X}{\partial \eta}+\frac{\partial Y}{\partial \xi}\cdot\frac{\partial Y}{\partial \eta} \quad .....(17)$$

$$\gamma=(\frac{\partial X}{\partial \xi})^2+(\frac{\partial Y}{\partial \xi})^2 \quad .....(18)$$

$$J=\frac{\partial X}{\partial \xi}\cdot\frac{\partial Y}{\partial \eta}-\frac{\partial X}{\partial \eta}\cdot\frac{\partial Y}{\partial \xi} \quad .....(19)$$

$$\phi=\frac{1}{J}\cdot(\frac{\partial X}{\partial \eta}(\alpha\cdot\frac{\partial^2 Y}{\partial \xi^2}-2\beta\cdot\frac{\partial^2 Y}{\partial \xi\partial \eta}+\gamma\frac{\partial^2 Y}{\partial \eta^2})-\frac{\partial Y}{\partial \eta}(\alpha\cdot\frac{\partial^2 X}{\partial \xi^2}-2\beta\cdot\frac{\partial^2 X}{\partial \xi\partial \eta}+\gamma\frac{\partial^2 X}{\partial \eta^2})) \quad .....(20)$$

$$\varepsilon=\frac{1}{J}\cdot(\frac{\partial Y}{\partial \xi}(\alpha\cdot\frac{\partial^2 X}{\partial \xi^2}-2\beta\cdot\frac{\partial^2 X}{\partial \xi\partial \eta}+\gamma\frac{\partial^2 X}{\partial \eta^2})-\frac{\partial X}{\partial \xi}(\alpha\cdot\frac{\partial^2 Y}{\partial \xi^2}-2\beta\cdot\frac{\partial^2 Y}{\partial \xi\partial \eta}+\gamma\frac{\partial^2 Y}{\partial \eta^2})) \quad .....(21)$$

The velocity components (U&V) given by equation (7) were rewritten in general coordinates and calculated from the following equations,[12]:

$$U=\frac{1}{J}\cdot(\frac{\partial X}{\partial \xi}\cdot\frac{\partial \psi}{\partial \eta}-\frac{\partial X}{\partial \eta}\cdot\frac{\partial \psi}{\partial \xi}) \quad .....(22)$$

$$V=\frac{1}{V}\cdot(\frac{\partial Y}{\partial \xi}\cdot\frac{\partial \psi}{\partial \eta}-\frac{\partial Y}{\partial \eta}\cdot\frac{\partial \psi}{\partial \xi}) \quad .....(23)$$

The heat transfer calculation within the cavity was obtained in terms of the average Nusselt number at the heated bottom surface. The heat transfer coefficient was expressed in dimensionless form by local Nusselt number. The definition of local Nusselt number in dimensionless differential form is, [13]:

$$Nu=-\frac{\partial \theta}{\partial n} \quad .....(24)$$

Where (n) is the coordinate normal to the surface.

The dimensionless form of local Nusselt number was also transformed to general coordinates (ζ,η), to be:

$$Nu=-\frac{1}{J\cdot\sqrt{\gamma}}(\gamma\cdot\frac{\partial \theta}{\partial \eta}-\beta\cdot\frac{\partial \theta}{\partial \xi}) \quad .....(25)$$

Setting the term $[(\partial\theta/\partial\xi)=0]$, as the temperature of the bottom surface was assumed to be constant the local Nusselt number became:

$$Nu=-\frac{\sqrt{\gamma}}{J}\cdot\frac{\partial \theta}{\partial \eta} \quad .....(26)$$

The average Nusselt number was obtained by integrating the local Nusselt number along the bottom surface using Simpson rule as follows:

$$\overline{Nu}=\frac{\int Nu\cdot ds}{S} \quad .....(27)$$

Where (s) represent the coordinate along the wavy surface.

4- Numerical Solution:

Numerical solutions for the governing equations with the associated boundary conditions were obtained using finite difference techniques. The nonlinear governing differential equations transformed to linear algebraic equations using finite difference discretization. The appropriate finite difference equation is written for each node, the residual for each node appears on the right hand side of the node equation. The elliptic stream function equation solved by successive over relaxation method (S.O.R), while the parabolic vorticity and energy equations are solved by (explicit) method.

A computer program is built to find the results. The calculations started with a suitable initial guessing and then it takes the previous iteration results as initial condition for the successive iteration. At each step, the solution is iterated until the normalized residuals become smaller than (0.0001).

5-Results and Discussion:

The results are carried out for a steady-state mixed convection in a square cavity with wavy upper and lower surfaces. In all cases the working fluid is air, the Prandtl number has been taken as (Pr=0.71). The effects of number of undulations of the upper and lower surfaces (λ) and its amplitude (A), the Richardson number and Grashof number on the fluid flow and heat transfer characteristics have been presented. In mixed convection, the effect of forced convection and its strength in comparison to natural convection can be judged on the base of Richardson number (Ri). When (Ri) approaches unity, the buoyancy effect becomes important. Consequently the natural convection dominates the mixed convection when (Ri>1). So, to allow combined effect of natural and forced convection, several cases are discussed in terms of streamlines, isotherms and Nusselt numbers for (Ri=0.01, 0.1, 1 &10), (λ=0 to 3), (A=0, 0.02, 0.04 & 0.06), (Gr=10^3 , $10^{3.5}$,10^4 & $10^{4.5}$).

5.1-Numerical Code Validation:

A computational model is validated for mixed convection heat transfer by comparing the results of local Nusselt number with that of the laminar mixed convection heat transfer in a square lid driven cavity with uniform bottom surface temperature performed by ref.[3]. In the present work, numerical predictions have been obtained for the same boundary conditions of ref.[3]. Figure (2) compares the results, it is seen that the agreement is good, so it can be decided that the current code can be used to predict the flow characteristics of the present study.

5.2 Effect of Number of Undulations of the Wavy Surfaces (λ):

The effect of number of undulations (λ) at a specified value of Richardson number (Ri=0.01) on streamlines and isotherms are studied at amplitude of undulation (A=0.04). Figure (3), (a_1 to d_1) show stream lines plots for different values of number of undulations (λ=0 to 3) at Gr=10^4 and Pr=0.71.

At low Richardson number (Ri=0.01), buoyancy effects are weak but accelerates the fluid near the lower heated surface resulting in low separation at the lower corners. The separation occurs at the corners of the opposite wall to the heated bottom surface. The separation near the upper surface increases as number of undulations (λ) increase which leads to decelerates the fluid at the upper cold surface.

The corresponding isotherm plots for the above cases are presented in the same figure (a_2 to d_2). For all cases, it can be observed that the thermal boundary layer thickness decreases at the left corner of the bottom hot surface and the right corner of the upper cold surface; this is revealed by the denser concentration of isotherms near these corners. While, at the other two corners the isothermal lines start to diverge from the upper and lower surface leading to a decrease in the heat transfer rate. However, despite this reduction in heat transfer, the temperature gradient increases.

Also it can be observed that increasing the number of undulation (λ) from 0 to 3 does not affect significantly the shape of streamlines and isotherms except that near the surfaces which takes nearly the shape of these surfaces.

5.3 The Effect of Amplitude of Undulations of the Wavy Surfaces:

Representative streamlines and isotherms plots are displayed in figure (4) (a_1 to d_1) & (a_2 to d_2), for different values of amplitude (A=0 to 0.06) at Ri=0.01, Pr=0.71, $Gr=10^4$ and $\lambda=3$. It is seen that increasing the value of (A) reduce the fluid circulation within the cavity, also the flow near the wavy surfaces is affected as the separation of streamlines and isotherms increases along these surfaces resulting in low heat transfer rates. In the region far away from the wavy surfaces, there is no effect on the shape of streamlines and isotherms associated to the increment of (A).

5.4 The Effect of Richardson number:

The effect of Richardson number (Ri) on streamlines and isotherms are studied at number of waves ($\lambda=3$) and amplitude of undulation (A=0.04). Figure (5), (a_1 to d_1) and (a_2 to d_2) show stream lines and isotherms plots for different values of Richardson number (Ri=0.01, 0.1, 1, 10) at $Gr=10^4$ and Pr=0.71.

It can be observed that at high Richardson number (Ri>1), the fluid accelerated resulting in low separation at the lower corners, the buoyancy effect becomes significant and the natural convection dominates the mixed convection resulting in low heat transfer rates.

Also it can be observed that increasing the Richardson number does not affect streamlines and isotherms pattern.

5.5 The Effect of Grashof number:

Streamlines and isotherms plots are presented in figure (6) (a_1 to d_1) & (a_2 to d_2) respectively, for different Grashof numbers ($Gr=10^3$ to $10^{4.5}$) at a number of waves ($\lambda=3$), amplitude of undulation (A=0.04), Richardson number (Ri=0.01) and Pr=0.71.

It can be observed that with increasing the Grashof number, the fluid accelerated as a result of increasing Reynolds number, resulting in low separation at the lower corners too. Also, the forced convection dominates the mixed convection and increases the heat transfer rates in contrast to increasing Richardson number which reduce that rate.

From the figure mentioned above it can be seen that, isotherm lines are nearly parallel for ($Gr=10^3$) which is similar to conduction-like distribution and starts to concentrate at the left corner of the lower hot surface and right corner of the upper cold surface and turns to diverge at the opposite corners for ($Gr > 10^3$) due to the dominating influence of the convective currents. At $Gr=10^4$ & $Gr=10^{4.5}$ convective distortion of the isotherms occurs throughout the cavity due to the strong influence of the convective current.

5.6 The Local and Mean Nusselt Number:

The heat transfer effectiveness of the cavity is displayed in terms of local Nusselt number values. The effects of varying (λ) on local Nusselt number along the heated surface are illustrated in figure (7), for amplitude value of (A=0.04), Ri=0.01, Pr=0.71 and $Gr=10^4$. As the flow develops and the bulk fluid gets heated, the maximum local Nusselt number increases from their lower values at ($\lambda=0$) to a higher values with increasing (λ). That is with increasing the number of waves the heat transfer rate increases. It is observed that the local Nusselt number for different (λ) shows an oscillatory phenomenon with increasing the number of waves of the heated surface (λ), because the vortex is not close enough to induce flow following the curving path of the concave parts of the wavy surface resulting in low heat transfer rates at those parts in comparison with convex parts of the surface.

The maximum Nusselt number distribution occur at the left corner of the lower surface due to high heat transfer rate, as the vortex is close enough to induce flow around the convex part of the first wave of the wavy lower surface and carry heat away, while the minimum Nusselt number distribution occur at the right corner due to low heat transfer rate as the isotherm lines diverges away from the surface.

The effect of variation of (A) on the local (Nu) at (Ri=0.01, $Gr=10^4$ & $\lambda=3$) are presented in figure (8). It is seen that the local Nusselt number for the whole surface, decreases with increasing

(A), except that for the small part of the heated lower surface near the left corner where the isotherm lines concentrated resulting in maximum value for the local Nusselt number at (A=0.04) which is greater than that at (A=0.06) for the same part. In general, a maximum value is deduced at (A=0.02), due to low resistance to fluid circulation within the cavity and low separation observed near the heated surface indicating that increasing the surface area of the wavy surface as a result of increasing the amplitude of undulation (A), does not increase the heat transfer rate as the effect on fluid circulation and separation dominates and reduce the heat transfer rate.

Figures (9 & 10) presented the effects of Richardson and Grashof numbers on the local Nusselt number, respectively, at the specified parameters. It is seen that the local Nusselt number for the whole surface, increases with increasing Grashof number and decreasing Richardson number for the reasons mentioned in paragraphs (5.4 &5.5).

The variation of the mean (Nu) with (λ) are presented in figure (11), for different values of (A). It is seen that the mean Nusselt number also decreases with increasing (A) and a maximum value is deduced at (A=0.02), for the same reason mentioned above.

For the same reason, it is seen that at low amplitudes of undulation (A=0&0.02), the mean Nusselt number profile is almost constant with (λ).

Figures (12 & 13) presented the variations of the mean (Nu) with (λ), for different values of Richardson number (Ri) and Grashof number (Gr), respectively. It is seen that the mean Nusselt number also increases with increasing (Gr) and decreasing (Ri) for the specified parameters mentioned in the figures, and a maximum value is deduced at ($Gr=10^{4.5}$ & Ri=0.01), for the same reasons mentioned previously.

6- Conclusions:

In this paper, mixed convection in cavity with wavy upper and lower surfaces is studied numerically. It is found that the heat transfer is strongly dependent on the number of waves (λ) and Grashof number (Gr) . The effects of increasing the amplitude of undulations (A) and Richardson number (Ri) are found to reduce the heat transfer within the cavity. In general, the local Nusselt number increases with increasing values of the number of waves (λ) and Grashof number (Gr) and decreases with increasing values of the amplitude of undulations (A) and Richardson number (Ri). Also the mean Nusselt number decreases with increasing values of the amplitude of undulations (A) and Richardson number (Ri) and increases with increasing Grashof number (Gr), maximum heat transfer occurs when the wavy surfaces designed with low amplitude of undulations. Higher mean Nusselt number is observed at (A=0.02 & $Gr=10^{4.5}$) at low Richardson number value (Ri=0.01). The validity of the numerical code is verified by comparison with published results. The result of the present work for the particular case (of changing Nusselt number with X) at a specified boundary conditions is in excellent agreement with those of the already published work by ref. [3] at the same boundary conditions.

Nomenclature:

A	Dimensionless height of wavy surface.
T	Temperature (^oK).
c,h	Subscripts denotes cold & hot.
g	Gravitational acceleration, (m/s^2).
Gr	Grashof number ($g\beta_e(T_h-T_c)\ H^3/\nu^2$).
H	Enclosure length.(m)
h	Convection heat transfer coefficient ($W/m^2.^oK$).
K	Effective thermal conductivity ($W/m.^oK$).
Nu	Nusselt number.
P	Dimensionless pressure.
Pr	Prandtl number (ν/α_e).
Re	Reynolds number (U_oH/ν).
Ri	Richardson number (Gr/Re^2).
U,V	Dimensionless velocities in X- & Y-direction.
U_o	Dimensionless free stream velocity.
u,v	Velocities in x- and y-direction, (m/s).
x,y	Cartesian coordinates.
X,Y	Dimensionless Cartesian coordinates.
ζ,η	Dimensionless computational coordinates.
α_e	Effective thermal diffusivity of fluid (m^2/s).
β_e	Coefficient of thermal expansion of fluid (K^{-1}).
ν	Kinematic viscosity of fluid (m^2/s).
ρ	Fluid density (kg/m^3).
θ	Dimensionless temperature $[(T-T_c)/(T_h-T_c)]$.
$\alpha,\beta,\gamma,J,\phi,\varepsilon$	Transforming coefficients to Body-Fitted Coordinates System.
λ	Number of waves.
φ	Stream function (m^2/s).
Ψ	Dimensionless stream function.
ω	Vorticity (1/s).
Ω	Dimensionless vorticity.

References:

1. Prasad A. K. and Koseff, J.R. "Combined forced and natural convection heat transfer in a deep lid-driven cavity flow", *Int. J. Heat and Fluid Flow*, Vol. 17, pp.460-467, 1996.
2. Khanafer, K.M. and Chamkha, A.J. "Mixed convection flow in a lid driven enclosure filled with a fluid-saturated porous medium", *Int. J. Heat Mass transfer,* Vol.42, pp.2465-2481, 1999.
3. Moallemi, M.K. and Jang, K.S. "Prandtl number effects on laminar mixed convection heat transfer in a lid driven cavity", *Int. J. Heat Mass transfer,* Vol.35, pp.1881-1892, 1992.
4. Iwatsu, R., Hyun, J.M. and Kuwahara, K. "Mixed convection in a driven cavity with a stable vertical temperature gradient", *Int. J. Heat Mass transfer,* Vol.36, pp.1601-1608, 1993.
5. Iwatsu, R. and Hyun, J.M."Three-dimensional driven cavity flows with a vertical temperature gradient", *Int. J. Heat Mass transfer,* Vol.38, pp.3319-3328, 1995.
6. Das, P.K.and Mahmud, S. "Numerical investigation of natural convection inside a wavy enclosure", *Int. J. Therm. Sci.* Vol. 42, pp.397-406, 2003.
7. Adjlout, L., Imine, O., Azzi, A. and Belkadi, M. "Laminar natural convection in an inclined cavity with a wavy wall", *Int. J. Heat & Mass Transfer,* Vol.45, pp.2141-2152, 2002.
8. Anderson, D.A., John, C., Tannehill and Richard,H. "*Computational Fluid Mechanics and Heat Transfer*", McGraw-Hill, 1997.

9. Anderson, D.A., John, C., "*Computational Fluid Dynamics;The Basic with Applications*", McGraw-Hill, 1995.
10. Thompson, J.F., Thames, F.C. and Mastin, C.W. "Automatic Numerical Generation of Body-Fitted Curvilinear Coordinate System for Field Containing any Number of Arbitrary Two-Dimensional Bodies.", *Journal of Computational Physics,* Vol. 15, pp.299-319, 1974.
11. Versteeg, H.K. and Malalasekera,W. "*An Introduction to computational fluid dynamics, the finite volume method",Longman scientific and technical,* John Whiley and Sons Inc., 1995.
12. Thames, F.C., Thompson, J.F., Mastin, C.W. and Walker, R.L. "Numerical solutions for Viscous and Potential Flow about Arbitrary Two-Dimensional Bodies Using Body-Fitted Coordinate Systems.", *Journal of Computational Physics,* Vol. 24, pp.245-273, 1977.
13. Holman, J.P. "*Heat Transfer*", McGRAW-HILL Kogakusha, Ltd., 1976.

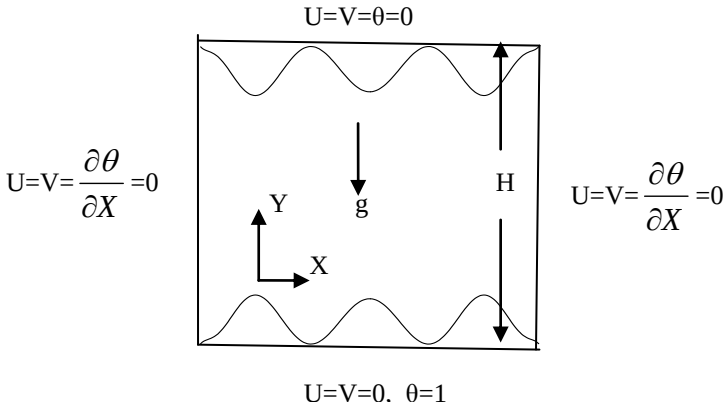

Fig.(1): Schematic diagram of the physical model.

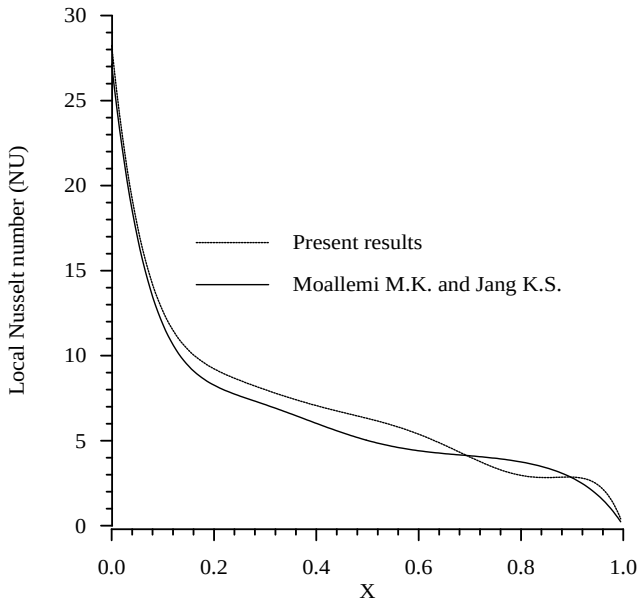

Fig.(2): Comparison of present results with other published results.

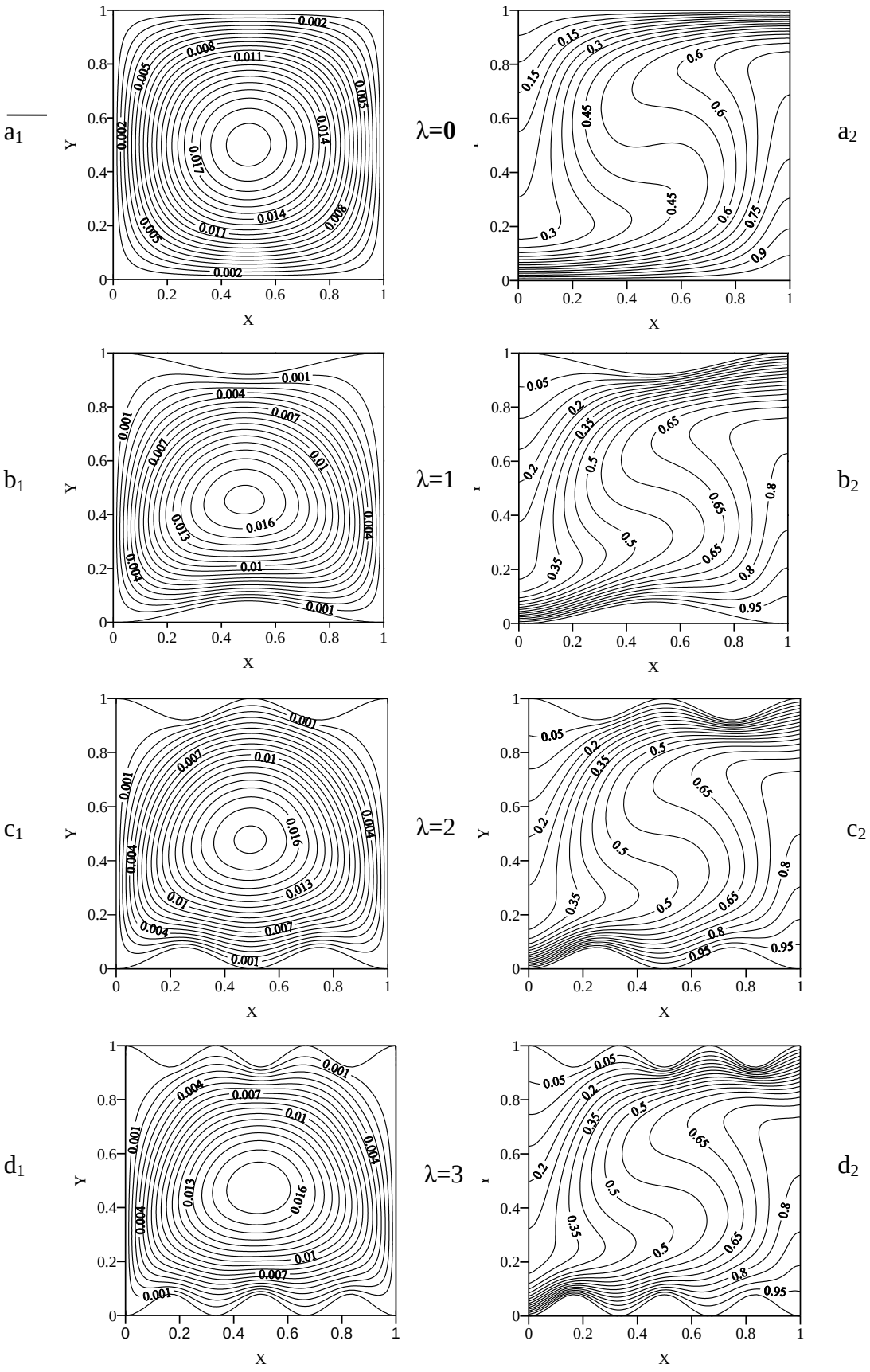

Fig.(3): Streamlines on the left and isotherms on the right for Ri=0.01, Pr=0.71, $Gr=10^4$ & A=0.04

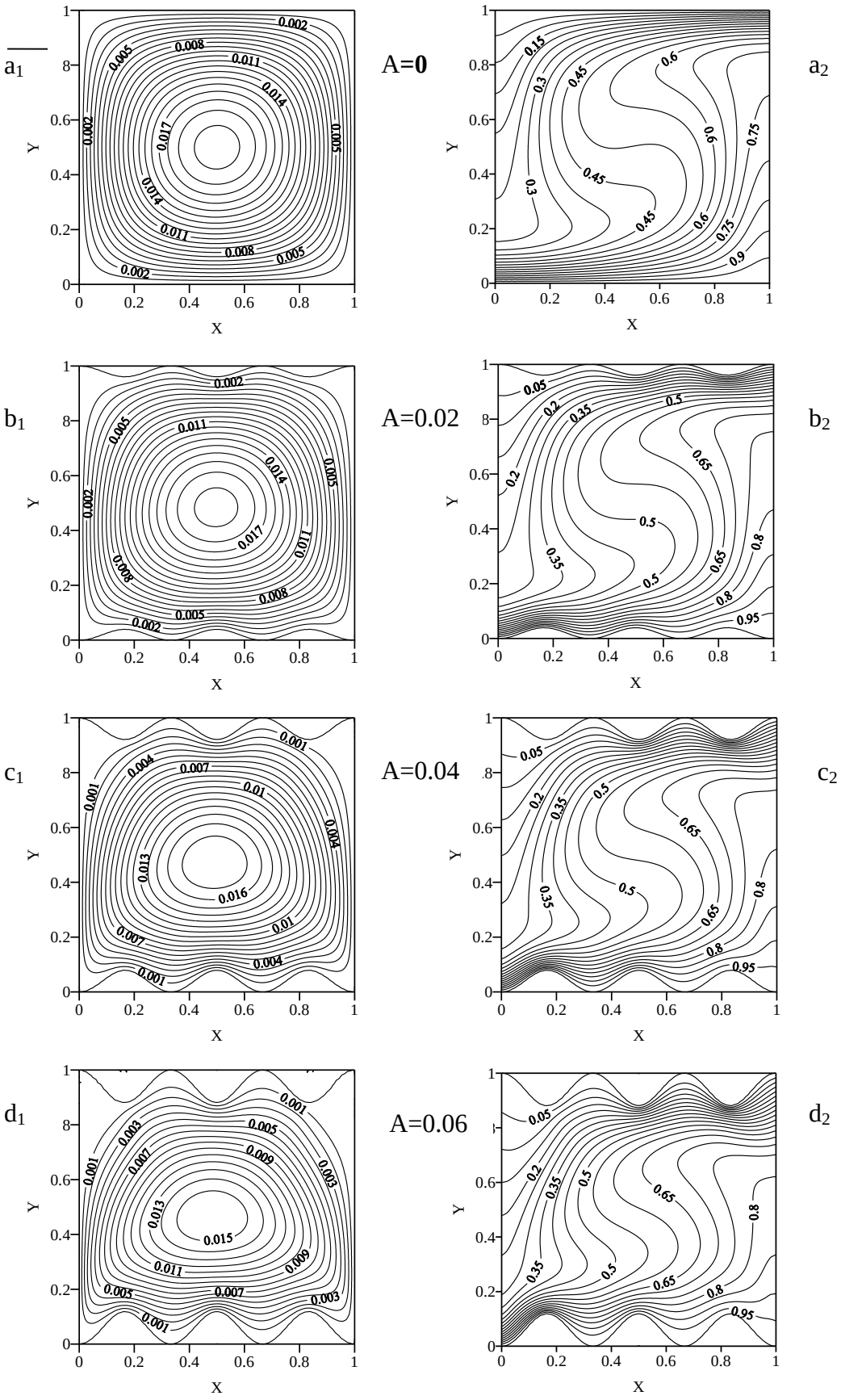

Fig.(4): Streamlines on the left and isotherms on the right for Ri=0.01, Pr=0.71, $Gr=10^4$ & $\lambda=3$.

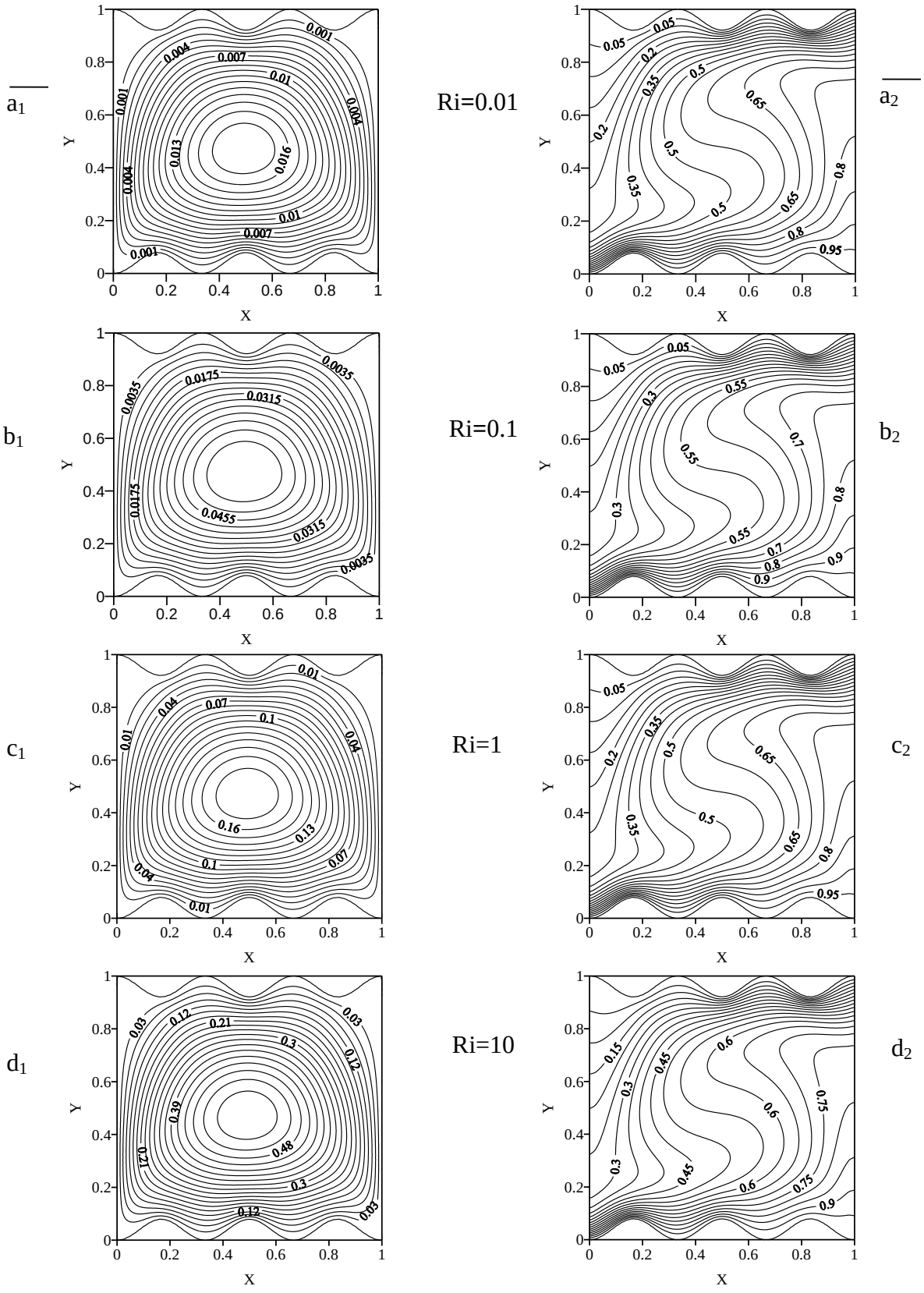

Fig.(5): Streamlines on the left and isotherms on the right for A=0.04, Pr=0.71, Gr=10^4 & λ=3.

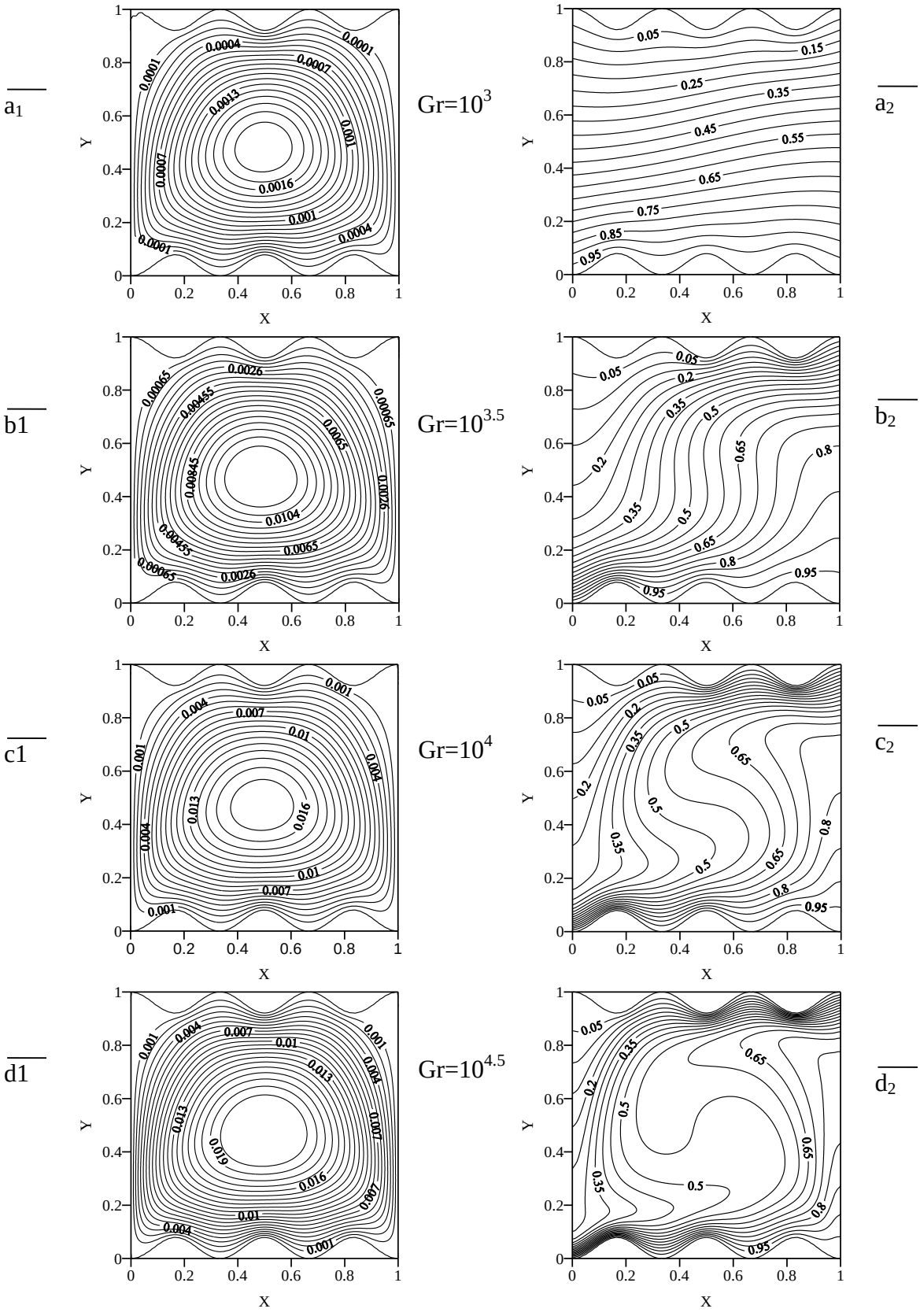

Fig.(6): Streamlines on the left and isotherms on the right for A=0.04, Pr=0.71, Ri=0.01 & λ=3.

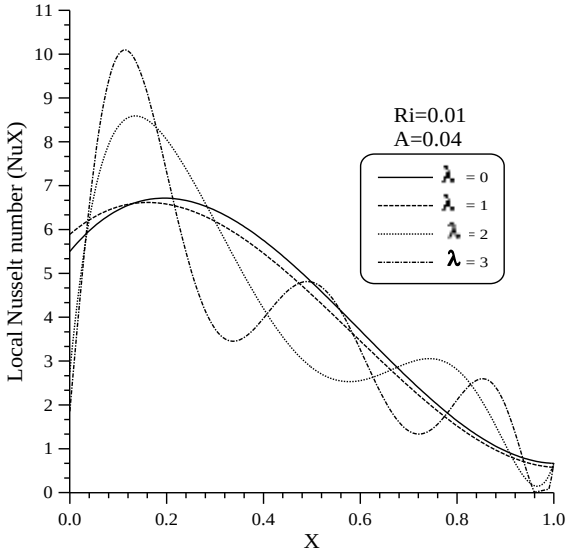

Fig.(7): The effect of number of waves on the local Nusselt number at Ri=0.01, $Gr=10^4$ and A=0.04

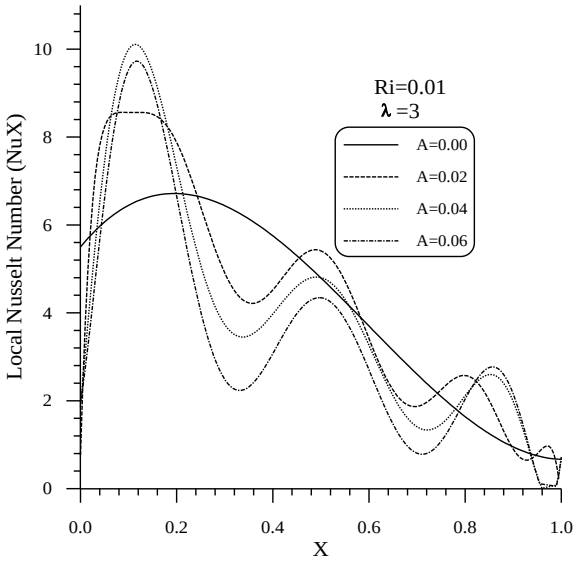

Fig.(8): The effect of amplitude of wavy surface on local Nusselt number at Ri=0.01, $Gr=10^4$ and λ =3.

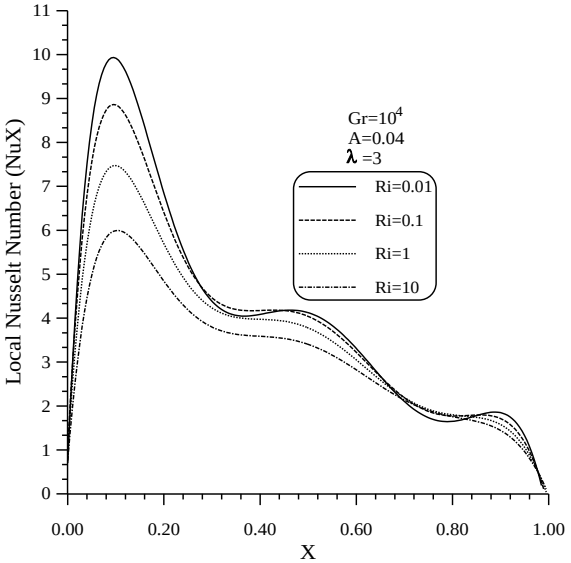

Fig (9):The effect of Richardson number on the local Nusselt number at A=0.04,$Gr=10^4$ and λ =3.

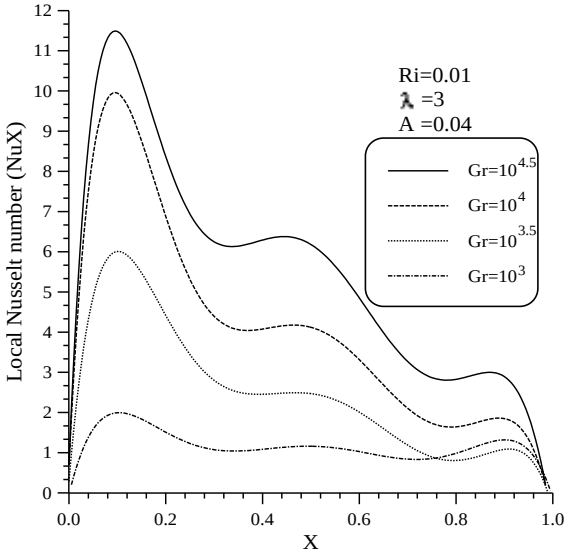

Fig.(10): The effect of Grashof number on the local Nusselt number at Ri=0.01, λ =3 and A=0.04

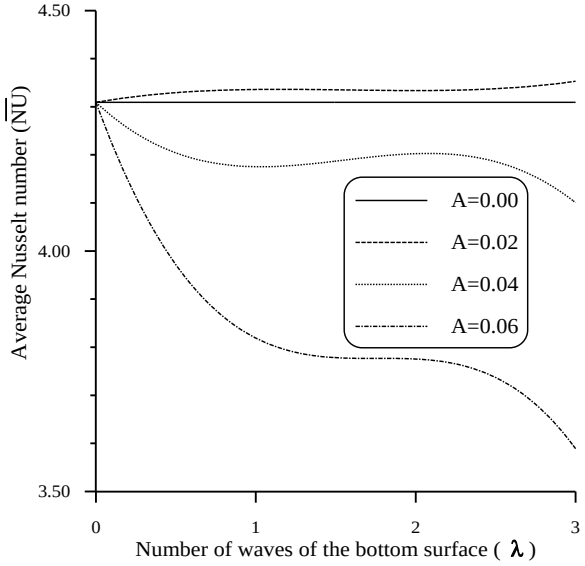

Fig.(11): The effect of amplitude of wavy surface on the average Nusselt number at Ri-0.01, $Gr=10^4$

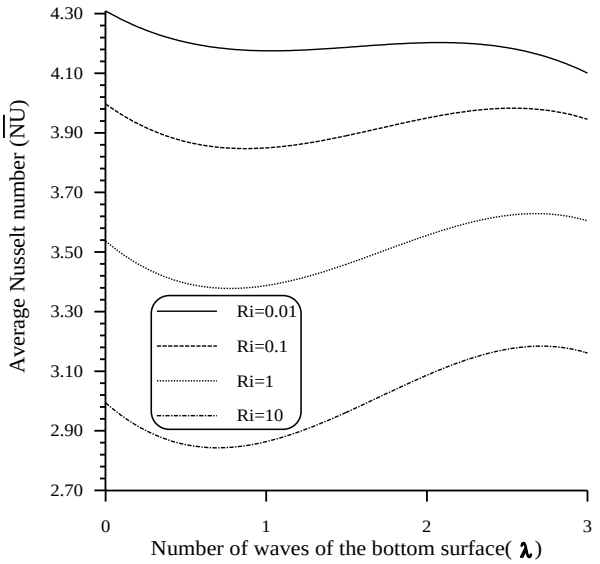

Fig.(12): The effect of Richardson number on the average Nusselt number at A=0.04, λ =3 & $Gr=10^4$

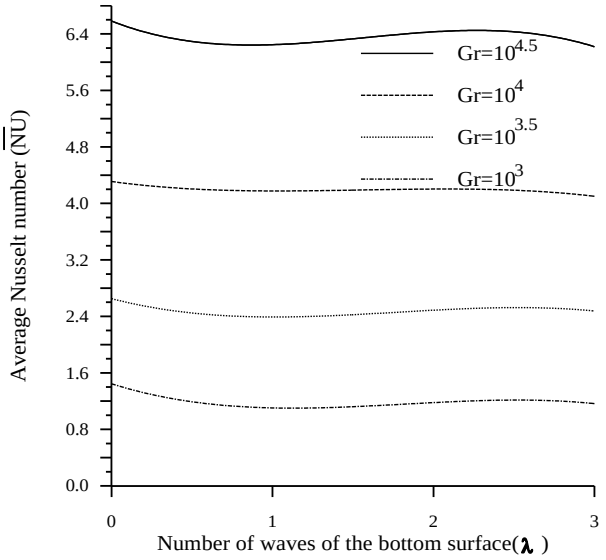

Fig.(13): The effect of Grashof number on the average Nusselt number at A=0.04, λ=3 & Ri=0.01.